SIAM J. SCI. COMPUT.
Vol. 36, No. 1, pp. A40–A62

FRACTIONAL SPECTRAL COLLOCATION METHOD*

MOHSEN ZAYERNOURI† AND GEORGE EM KARNIADAKIS†

Abstract. We develop an exponentially accurate fractional spectral collocation method for solving steady-state and time-dependent fractional PDEs (FPDEs). We first introduce a new family of interpolants, called *fractional Lagrange interpolants*, which satisfy the Kronecker delta property at collocation points. We perform such a construction following a spectral theory recently developed in [M. Zayernouri and G. E. Karniadakis, *J. Comput. Phys.*, 47 (2013), pp. 2108–2131] for fractional Sturm–Liouville eigenproblems. Subsequently, we obtain the corresponding fractional differentiation matrices, and we solve a number of linear FODEs in addition to linear and nonlinear FPDEs to investigate the numerical performance of the fractional collocation method. We first examine space-fractional advection-diffusion problem and generalized space-fractional multiterm FODEs. Next, we solve FPDEs, including the time- and space-fractional advection-diffusion equation, time- and space-fractional multiterm FPDEs, and finally the space-fractional Burgers equation. Our numerical results confirm the exponential convergence of the fractional collocation method.

Key words. polyfractonomial basis functions, fractional Lagrange interpolants, fractional differentiation matrix, FODEs, FPDEs, exponential convergence

AMS subject classifications. 58C40, 35S10, 35S11, 65M70

DOI. 10.1137/130933216

1. Introduction.

The notion of fractional calculus and differential operators of fractional order appear in modeling diverse physical systems such as viscous fluid flows due to the *cumulative memory* effect of wall-friction [5, 13, 31], porous or fractured media [2], bioengineering applications [25], and viscoelastic materials [26]. In addition, it has been found that the transport dynamics in complex systems is governed by *anomalous* diffusion demonstrating nonexponential relaxation patterns [4, 27, 16]. The governing equation of evolution for the probability density function of such non-Markovian processes turns out to be a time-fractional diffusion equation. The notion of fractional derivatives has been rapidly extended to many fractional partial differential equations (FPDEs), such as the fractional Burgers equation [30], the fractional Fokker–Planck equation [1], the fractional advection-diffusion equation [10], and fractional-order multiterm equations [22].

The extension of existing numerical methods for integer-order differential equations ([9, 18, 11, 35, 12] and references therein) to their corresponding fractional differential equations is not trivial. The main challenge in simulation of fractional-order systems is that the approximation of these models is computationally demanding due to their long-range *history* dependence. However, the development of numerical schemes in this area does not have a long history and has recently undergone a fast evolution.

The idea of discretized fractional calculus within the spirit of the finite difference method (FDM) was introduced by Lubich [23, 24]. Sanz-Serna [29] adopted the

*Submitted to the journal's Methods and Algorithms for Scientific Computing section August 16, 2013; accepted for publication (in revised form) October 30, 2013; published electronically January 14, 2014. This work was supported by the Collaboratory on Mathematics for Mesoscopic Modeling of Materials (CM4) at PNNL, funded by the Department of Energy, by OSD/MURI, and by NSF/DMS.
http://www.siam.org/journals/sisc/36-1/93321.html

†Division of Applied Mathematics, Brown University, Providence, RI 02912 (mohsen_zayernouri@brown.edu, george_karniadakis@brown.edu).

idea of Lubich and presented a temporal semidiscrete algorithm for partial integro-differential equations, which was first-order accurate. Sugimoto [30] also employed an FDM for approximating the fractional derivative in Burgers equation. The paper of Metzler and Klafter [27] opened a new chapter in FPDEs, where a fractional dynamics approach to time-fractional diffusion was introduced. Subsequently, Gorenflo et al. [8] adopted a finite difference scheme by which they could generate discrete models of random walk in such anomalous diffusion. At this time, Diethelm and others proposed a predictor-corrector scheme in [6, 7] in addition to a fractional Adams method. Next, Langlands and Henry [17] considered the fractional diffusion equation and analyzed the L^1 scheme for the time-fractional derivative. Sun and Wu [32] also constructed a difference scheme approximation of a time-fractional derivative with order $(2-\alpha)$. The FDM is inherently a *local* approach, whereas fractional derivatives are essentially *global* (nonlocal) differential operators. Hence, although the implementation of such FDM approaches is relatively easy, the big challenge in such schemes is their limited accuracy. Moreover, these approaches suffer from a high cost of computing the long-range memory in discretization of the fractional derivatives at each point. This challenge would suggest that global schemes such as *spectral methods* are more appropriate tools for discretizing fractional differential equations.

Compared to the extensive amount of work put into developing FDM schemes in the literature, only a little effort has been put into developing global and high-order spectral methods based on a rigorous framework. A Fourier spectral method was utilized by Sugimoto [30] in a fractional Burgers equation, and a spline-based collocation method was employed by Blank [3]. In these works, the expected high convergence rate was not observed and no error or stability analysis were carried out. Lin and Xu [21] developed a hybrid scheme for time-fractional diffusion problem, treating the time-fractional derivative using FDM and discretizing the *integer-order* spatial derivative by a Legendre spectral method. In such mixed approaches, the error associated with the low-order temporal accuracy can easily dominate the global error.

The first rigorous work on spectral methods for FPDEs was published by Li and Xu [19, 20], who developed a time-space spectral method for the time-fractional diffusion equation. They achieved *exponential* convergence in their numerical tests in agreement with their error analysis. However, in this scheme, the corresponding stiffness and mass matrices are dense and gradually become ill-conditioned when the fractional order α tends to small values. Moreover, treatment of multiterm FPDEs and nonlinear FPDEs is not easy using this approach, and there is no straightforward variational form for such problems in general. Recently, Zayernouri and Karniadakis have developed exponentially accurate spectral and discontinuous *hp*-spectral element methods of Petrov–Gaerkin (PG) type for fractional differential equations [34]. These methods are developed based on the fractional Sturm–Liouville eigenproblems (FSLPs) [33]. They are not only exponentially fast but also are based on a nice variational framework, so one can perform standard stability and error analyses for such methods.

Galerkin/PG projection type schemes in general have difficulties in the treatment of nonlinear FPDEs and multiterm FPDEs, since no straightforward variational form can be efficiently obtained for such problems. The *collocation* schemes for fractional equations are relatively easy to implement and they can overcome the aforementioned challenges. The idea of collocation was proposed by Khader in [14], who presented a Chebyshev collocation method for the discretization of the space-fractional diffusion equation. More recently, Khader and Hendy [15] developed a Legendre pseudospectral

method for fractional-order delay differential equations. However, in these works only linear problems have been considered and the performance of such methods has not been fully investigated.

The aim of this study is to develop an exponentially accurate fractional spectral collocation method (FSCM) for solving steady-state and time-dependent FPDEs. The organization of the paper is as follows. In section 2, we begin with some preliminary definitions of fractional calculus. In section 3, we introduce *fractional Lagrange interpolants*, which satisfy the Kronecker delta property at collocation points. Moreover, we obtain the corresponding fractional differentiation matrices. In section 4, we solve a number of linear and nonlinear FPDEs to investigate the numerical performance of the fractional collocation method. In this section, we examine steady-state problems such as the space-fractional advection-diffusion and generalized space-fractional multiterm problems, in addition to time-dependent FPDEs such as the time- and space-fractional advection-diffusion equation, time- and space- fractional multiterm FPDEs, and finally the space-fractional Burgers equation. We demonstrate the exponential convergence of FSCM. We end the paper with a summary and discussion in section 5, where we discuss the performance of FSCM. We show that among other high-order methods and finite difference schemes, our FSCM scheme has a number of advantages, including ease of implementation, lower computational cost, and exponential accuracy.

2. Notation and definitions. Before presenting our FSCM, we start with some preliminary definitions of fractional calculus [28]. The left-sided and right-sided Riemann–Liouville fractional derivatives of order μ, when $0 < \mu < 1$, are defined as

$$({}^{RL}_{-1}\mathcal{D}^{\mu}_{x} f)(x) = \frac{1}{\Gamma(1-\mu)} \frac{d}{dx} \int_{-1}^{x} \frac{f(s)ds}{(x-s)^{\mu}}, \quad x > -1, \tag{2.1}$$

and

$$({}^{RL}_{x}\mathcal{D}^{\mu}_{1} f)(x) = \frac{1}{\Gamma(1-\mu)} \left(\frac{-d}{dx}\right) \int_{x}^{1} \frac{f(s)ds}{(s-x)^{\mu}}, \quad x < 1. \tag{2.2}$$

Furthermore, the corresponding left- and right-sided Caputo derivatives of order $\mu \in (0,1)$ are obtained as

$$({}^{C}_{-1}\mathcal{D}^{\mu}_{x} f)(x) = \frac{1}{\Gamma(1-\mu)} \int_{-1}^{x} \frac{f'(s)ds}{(x-s)^{\mu}}, \quad x > -1, \tag{2.3}$$

and

$$({}^{C}_{x}\mathcal{D}^{\mu}_{1} f)(x) = \frac{1}{\Gamma(1-\mu)} \int_{-1}^{x} \frac{-f'(s)ds}{(x-s)^{\mu}}, \quad x < 1. \tag{2.4}$$

The two definitions of fractional derivatives of Riemann–Liouville and Caputo type are closely linked by the following relationship:

$$({}^{RL}_{-1}\mathcal{D}^{\mu}_{x} f)(x) = \frac{f(-1)}{\Gamma(1-\mu)(x+1)^{\mu}} + ({}^{C}_{-1}\mathcal{D}^{\mu}_{x} f)(x), \tag{2.5}$$

and

$$({}^{RL}_{x}\mathcal{D}^{\mu}_{1} f)(x) = \frac{f(1)}{\Gamma(1-\mu)(1-x)^{\mu}} + ({}^{C}_{x}\mathcal{D}^{\mu}_{1} f)(x). \tag{2.6}$$

We also recall a useful property of the Riemann–Liouville fractional derivatives. Assume that $0 < p \leq 1$ and $0 < q \leq 1$ and $f(-1) = 0 \;\; x > -1$; then

$$ {}^{RL}_{-1}\mathcal{D}_x^{p+q} f(x) = \left({}^{RL}_{-1}\mathcal{D}_x^{p}\right)\left({}^{RL}_{-1}\mathcal{D}_x^{q}\right) f(x) = \left({}^{RL}_{-1}\mathcal{D}_x^{q}\right)\left({}^{RL}_{-1}\mathcal{D}_x^{p}\right) f(x). \tag{2.7} $$

Finally, from [28] and for $\mu \in (0,1)$, we have

$$ {}^{C}_{0}\mathcal{D}_x^{\mu} x^k = \begin{cases} 0, & k < \mu, \\ \frac{\Gamma(k+1)}{\Gamma(k+1-\mu)} x^{k-\mu}, & 0 < \mu \leq k. \end{cases} \tag{2.8} $$

In this paper, we deal with fractional problems with *homogeneous* boundary/initial conditions. Hence, from now on, we drop the type of the fractional derivative and represent them by $\mathcal{D}^{\mu}$. Clearly, any problem with nonhomogeneous boundary/initial conditions can be converted to a corresponding homogeneous one through (2.5) and (2.6).

3. Fractional Lagrange interpolants. In standard collocation methods, interpolation operators are the key to circumvent the need for evaluating the inner products in Galerkin and PG-type spectral methods. To this end, we define a set of *interpolation points* $\{x_i\}_{i=1}^{N}$ on which the corresponding Lagrange interpolants are obtained. Moreover, to form a collocation method, we require the residual to vanish on the same set of grid points, called *collocation points* $\{y_i\}_{i=1}^{N}$. In general, these residual-vanishing points do not need to be same as the interpolation points. Our fractional collocation scheme is inspired by a new spectral theory developed for FSLPs in [33], by which we solve

$$ \begin{aligned} {}_0\mathcal{D}_t^{\tau} u(x,t) &= \mathcal{L}^{\nu} u(x,t), \quad x \in [-1,1], \; t \in [0,T], \\ u(x,0) &= g(x), \\ u(-1,t) &= 0, \quad \nu \in (0,1), \\ u(-1,t) = u(1,t) &= 0, \quad \nu \in (1,2), \end{aligned} \tag{3.1} $$

in which $\tau \in (0,1)$ and $\mathcal{L}^{\nu}$ denotes a fractional differential operator, where ν denotes the highest fractional order. We represent the solution to (3.1) in terms of new fractal (nonpolynomial) basis functions, called *Jacobi polyfractonomials*, which are the eigenfunctions of the FSLP of the first kind, explicitly obtained as

$$ {}^{(1)}\mathcal{P}_n^{\alpha,\beta,\mu}(x) = (1+x)^{-\beta+\mu-1} P_{n-1}^{\alpha-\mu+1,-\beta+\mu-1}(x), \quad x \in [-1,1], \tag{3.2} $$

where $P_{n-1}^{\alpha-\mu+1,-\beta+\mu-1}(x)$ are the standard Jacobi polynomials in which $\mu \in (0,1)$, $-1 \leq \alpha < 2-\mu$, and $-1 \leq \beta < \mu - 1$. It has been shown that eigenfunctions with $\alpha = \beta$ exhibit identical approximating properties when they are utilized as basis functions. Hence, we consider the polyfractonomial eigenfunctions corresponding to $\alpha = \beta = -1$ as

$$ {}^{(1)}\mathcal{P}_n^{\mu}(x) = (1+x)^{\mu} P_{n-1}^{-\mu,\mu}(x), \quad x \in [-1,1]. \tag{3.3} $$

From the properties of the eigensolutions in [33], the left-sided fractional derivative of (3.3), of both Riemann–Liouville and Caputo sense, is given as

$$ {}_{-1}\mathcal{D}_x^{\mu}\left({}^{(1)}\mathcal{P}_n^{\mu}(x)\right) = \frac{\Gamma(n+\mu)}{\Gamma(n)} P_{n-1}(x), \tag{3.4}$$

where $P_{n-1}(x)$ denotes a Legendre polynomial of order $(n-1)$. In our fractional collocation method, we seek solutions

$$ u_N \in V_N^{\mu} = span\{{}^{(1)}\mathcal{P}_n^{\mu}(x), 1 \le n \le N\}, \tag{3.5}$$

$\mu \in (0,1), x \in [-1,1]$, of the form

$$ u_N(x) = \sum_{j=1}^{N} \hat{u}_j \ {}^{(1)}\mathcal{P}_j^{\mu}(x). \tag{3.6}$$

This polyfractonomial *modal* expansion can also be alternatively expressed as a *nodal* expansion as

$$ u_N(x) = \sum_{j=1}^{N} u_N(x_j)\, h_j^{\mu}(x), \tag{3.7}$$

where $h_j^{\mu}(x)$ represent *fractional Lagrange interpolants* and are defined using the aforementioned interpolations points $-1 = x_1 < x_2 < \cdots < x_N = 1$. The interpolants $h_j^{\mu}(x)$ are all of fractional order $(N+\mu-1)$ and are defined as

$$ h_j^{\mu}(x) = \Big(\frac{x-x_1}{x_j-x_1}\Big)^{\mu} \prod_{\substack{k=1 \\ k\neq j}}^{N} \Big(\frac{x-x_k}{x_j-x_k}\Big), \ \ 2 \le j \le N. \tag{3.8}$$

Here, we call the superscript μ *interpolation parameter* to be set prior to solving (3.1). We note that a general FPDE, however, can be associated with multiple fractional differentiation orders ν_k, $k = 1, 2, \ldots, K$, for some positive integer K. We shall show how to set μ just from the fractional orders ν_k, given in the problem.

Remark 1. Because of the homogeneous Dirichlet boundary condition(s) in (3.1), we only construct $h_j^{\mu}(x)$ for $j = 2, 3, \ldots, N$ when maximum fractional order $\nu \in (0,1)$, for which we set $u_N(-1) = 0$. Moreover, when $\nu \in (1,2)$, there are only $(N-2)$ fractional Lagrange interpolants $h_j^{\mu}(x)$, $j = 2, 3, \ldots, N-1$, to construct since we impose $u_N(\pm 1) = 0$.

The fractional interpolants, shown in (3.8), satisfy the Kronecker delta property, i.e., $h_j^{\mu}(x_k) = \delta_{jk}$, at interpolation points; however, they vary as a polyfractonomial between x_k's. We employ these interpolants as fractional *nodal* basis functions in (3.7), where they mimic the key structure of the eigenfunctions (3.3), utilized as fractional *modal* bases in the expansion (3.6).

3.1. Fractional differentiation matrix $\boldsymbol{D^{\sigma}}$, $\boldsymbol{0 < \sigma < 1}$. Next, we obtain the differentiation matrix $\mathbf{D}^{\sigma}$ of a general fractional order $\sigma \in (0,1)$. We substitute (3.8) in (3.7) and take the σth order fractional derivative as

$$
\begin{aligned}
(3.9)\qquad {}_{-1}\mathcal{D}_x^{\sigma} u_N(x) &= {}_{-1}\mathcal{D}_x^{\sigma}\left[\sum_{j=2}^{N} u_N(x_j)\, h_j^{\mu}(x)\right] \\
&= \sum_{j=2}^{N} u_N(x_j)\ {}_{-1}\mathcal{D}_x^{\sigma}\left[h_j^{\mu}(x)\right] \\
&= \sum_{j=2}^{N} u_N(x_j)\ {}_{-1}\mathcal{D}_x^{\sigma}\left[\left(\frac{x-x_1}{x_j-x_1}\right)^{\mu}\prod_{\substack{k=1\\k\neq j}}^{N}\left(\frac{x-x_k}{x_j-x_k}\right)\right] \\
&= \sum_{j=2}^{N} u_N(x_j)\ {}_{-1}\mathcal{D}_x^{\sigma}\left[(1+x)^{\mu}\mathcal{G}_j\right] a_j,
\end{aligned}
$$

where $a_j = \frac{1}{(x_j-x_1)^{\mu}}$, and $\mathcal{G}_j = \prod_{\substack{k=1\\k\neq j}}^{N}(\frac{x-x_k}{x_j-x_k})$, $j = 2,3,\ldots,N$, are all polynomials of order $(N-1)$, which can be represented exactly in terms of Jacobi polynomials $P_{n-1}^{-\mu,\mu}(x)$ as

$$
(3.10)\qquad \mathcal{G}_j = \sum_{n=1}^{N} \beta_n^j P_{n-1}^{-\mu,\mu}(x).
$$

We note that the unknown coefficients β_n^j can be obtained analytically. Plugging (3.10) into (3.9), we obtain

$$
\begin{aligned}
(3.11)\qquad {}_{-1}\mathcal{D}_x^{\mu} u_N(x) &= \sum_{j=2}^{N} u_N(x_j)\ {}_{-1}\mathcal{D}_x^{\sigma}\left[(1+x)^{\mu}\sum_{n=1}^{N}\beta_n^j P_{n-1}^{-\mu,\mu}(x)\right] a_j \\
&= \sum_{j=2}^{N} u_N(x_j) a_j \sum_{n=1}^{N}\beta_n^j\ {}_{-1}\mathcal{D}_x^{\sigma}\left[(1+x)^{\mu} P_{n-1}^{-\mu,\mu}(x)\right] \text{ by (3.3)}, \\
&= \sum_{j=2}^{N} u_N(x_j) a_j \sum_{n=1}^{N}\beta_n^j\ {}_{-1}\mathcal{D}_x^{\sigma}\left[\,{}^{(1)}\mathcal{P}_n^{\mu}(x)\right] \text{ by (3.4)}.
\end{aligned}
$$

(I) The particular case $\sigma = \mu \in (0,1)$. In this case, we use the property (3.4) and obtain

$$
(3.12)\qquad {}_{-1}\mathcal{D}_x^{\sigma} u_N(x) = \sum_{j=2}^{N} u_N(x_j) a_j \sum_{n=1}^{N}\beta_n^j\left[\frac{\Gamma(n+\mu)}{\Gamma(n)} P_{n-1}(x)\right].
$$

Consequently, we take the interpolation and collocation points to be identical, also recalling Remark 1 and by evaluating ${}_{-1}\mathcal{D}_x^{\mu} u_N(x)$ at the collocation points $\{x_i\}_{i=2}^{N}$ we obtain

$$
\begin{aligned}
(3.13)\qquad {}_{-1}\mathcal{D}_x^{\mu} u_N(x)\Big|_{x_i} &= \sum_{j=2}^{N} u_N(x_j) a_j \sum_{n=1}^{N}\beta_n^j\left[\frac{\Gamma(n+\mu)}{\Gamma(n)} P_{n-1}(x_i)\right], \\
&= \sum_{j=2}^{N} \mathbf{D}_{ij}^{\mu}\ u_N(x_j),
\end{aligned}
$$

where $\mathbf{D}^{\mu}_{ij}$ are the entries of the $(N-1)\times(N-1)$ *fractional differentiation matrix* $\mathbf{D}^{\mu}$, obtained as

$$\mathbf{D}^{\mu}_{ij} = \frac{1}{(x_j+1)^{\mu}} \sum_{n=1}^{N} \frac{\Gamma(n+\mu)}{\Gamma(n)}\, \beta^j_n\, P_{n-1}(x_i). \tag{3.14}$$

(II) The general case $\sigma \in (0,1)$. This case is important when the fractional differential operator is associated with multiple fractional derivatives of different order. To obtain the fractional differentiation matrix in this case, we perform an affine mapping from $x \in [-1,1]$ to $s \in [0,1]$ through $s = (x+1)/2$ and rewrite (3.11) as

$$\begin{aligned} {}_{-1}\mathcal{D}_x^{\sigma} u_N(x) &= \sum_{j=2}^{N} u_N(x_j) a_j \sum_{n=1}^{N} \beta^j_n\ {}_{-1}\mathcal{D}^{\sigma}_{x(s)} \Big[{}^{(1)}\mathcal{P}_n^{\mu}(x(s)) \Big], \\ &= \sum_{j=2}^{N} u_N(x_j) a_j \sum_{n=1}^{N} \beta^j_n \left(\frac{1}{2}\right)^{\sigma}\ {}_0\mathcal{D}_s^{\sigma} \Big[{}^{(1)}\mathcal{P}_n^{\mu}(x(s)) \Big], \end{aligned} \tag{3.15}$$

where ${}^{(1)}\mathcal{P}_n^{\mu}(x(s))$ denotes the *shifted basis* that can be represented as

$${}^{(1)}\mathcal{P}_n^{\mu}(x(s)) = 2^{\mu} \sum_{q=0}^{n-1} (-1)^{n+q-1} \binom{n-1+q}{q} \binom{n-1+\mu}{n-1-q} s^{q+\mu}. \tag{3.16}$$

Substituting (3.16) into (3.15) we have

$$\begin{aligned} &{}_{-1}\mathcal{D}_x^{\sigma} u_N(x) \\ &\quad = 2^{\mu-\sigma} \sum_{j=2}^{N} u_N(x_j) a_j \sum_{n=1}^{N} \beta^j_n \sum_{q=0}^{n-1} (-1)^{n+q-1} \binom{n-1+q}{q} \binom{n-1+\mu}{n-1-q}\, {}_0\mathcal{D}_s^{\sigma} \Big[s^{q+\mu} \Big], \end{aligned}$$

in which ${}_0\mathcal{D}_s^{\sigma}\big[s^{q+\mu}\big]$ can be evaluated exactly by (2.8), and finally by an inverse transformation we obtain the σ-fractional derivative of the approximate solution as

$${}_{-1}\mathcal{D}_x^{\sigma} u_N(x) = \sum_{j=2}^{N} u_N(x_j) \left[a_j \sum_{n=1}^{N} \beta^j_n \sum_{q=\lceil \sigma-\mu \rceil}^{n-1} b_{nq}\, (x+1)^{q+\mu-\sigma} \right], \tag{3.17}$$

in which $\lceil \sigma-\mu \rceil$ denotes the ceiling of $\sigma-\mu$ and

$$b_{nq} = (-1)^{n+q-1} \left(\frac{1}{2}\right)^{q} \binom{n-1+q}{q} \binom{n-1+\mu}{n-1-q} \frac{\Gamma(q+\mu+1)}{\Gamma(q+\mu-\sigma+1)}. \tag{3.18}$$

Now, similarly by evaluating ${}_{-1}\mathcal{D}_x^{\mu} u_N(x)$ at the collocation points $\{x_i\}_{i=2}^{N}$,

$$\begin{aligned} {}_{-1}\mathcal{D}_x^{\sigma} u_N(x)\Big|_{x_i} &= \sum_{j=2}^{N} u_N(x_j) \left[a_j \sum_{n=1}^{N} \beta^j_n \sum_{q=\lceil \sigma-\mu \rceil}^{n-1} b_{nq}\, (x_i+1)^{q+\mu-\sigma} \right], \\ &= \sum_{j=2}^{N} \mathbf{D}^{\sigma}_{ij}\ u_N(x_j), \end{aligned} \tag{3.19}$$

where $\mathbf{D}^{\sigma}_{ij}$ are the entries of the $(N-1)\times(N-1)$ fractional differentiation matrix $\mathbf{D}^{\sigma}$, computed as

$$\mathbf{D}^{\sigma}_{ij} = \frac{1}{(x_j+1)^{\mu}} \sum_{n=1}^{N} \beta^j_n \sum_{q=\lceil \sigma-\mu \rceil}^{n-1} b_{nq}\, (x_i+1)^{q+\mu-\sigma}. \tag{3.20}$$

3.2. Fractional differentiation matrix $D^{1+\sigma}$, $0 < \sigma < 1$. As before, we split the derivation into two parts.

(I) The particular case $\sigma = \mu$. The fractional derivative matrix $\mathbf{D}^{1+\sigma}$ when $\sigma = \mu$ can be directly obtained following (2.7) and by taking the first derivative of (3.12) as

$$\begin{aligned}
{}_{-1}\mathcal{D}_x^{1+\mu} u_N(x) &= \frac{d}{dx}\Big[{}_{-1}\mathcal{D}_x^{\mu} u_N(x)\Big] \\
&= \frac{d}{dx}\sum_{j=2}^{N} u_N(x_j) a_j \sum_{n=1}^{N} \beta_n^j \left[\frac{\Gamma(n+\mu)}{\Gamma(n)} P_{n-1}(x)\right] \\
&= \sum_{j=2}^{N} u_N(x_j) a_j \sum_{n=1}^{N} \beta_n^j \left[\frac{\Gamma(n+\mu)}{\Gamma(n)} \frac{dP_{n-1}(x)}{dx}\right] \\
&= \sum_{j=1}^{N} u_N(x_j) a_j \sum_{n=2}^{N} \beta_n^j \left[\frac{\Gamma(n+\mu)}{\Gamma(n)} \frac{n}{2} P_{n-2}^{1,1}(x)\right].
\end{aligned}$$

Similarly, we can evaluate ${}_{-1}\mathcal{D}_x^{1+\mu} u_N(x)$ at the collocation points $\{x_i\}_{i=1}^N$ to obtain

$$\begin{aligned}
{}_{-1}\mathcal{D}_x^{1+\mu} u_N(x)\Big|_{x_i} &= \sum_{j=1}^{N} u_N(x_j) a_j \sum_{n=2}^{N} \beta_n^j \left[\frac{\Gamma(n+\mu)}{\Gamma(n)} \frac{n}{2} P_{n-2}^{1,1}(x_i)\right] \\
&= \sum_{j=1}^{N} \mathbf{D}_{ij}^{1+\mu}\, u_N(x_j),
\end{aligned} \tag{3.21}$$

where $\mathbf{D}_{ij}^{1+\mu}$ are the entries of the fractional differentiation matrix $\mathbf{D}^{1+\mu}$, provided as

$$\mathbf{D}_{ij}^{1+\mu} = \frac{1}{(x_j+1)^{\mu}} \sum_{n=2}^{N} \beta_n^j \left[\frac{\Gamma(n+\mu)}{\Gamma(n)} \frac{n}{2} P_{n-2}^{1,1}(x_i)\right]. \tag{3.22}$$

(II) Case $\sigma \neq \mu$. For the case $\sigma \neq \mu$, it suffices to take the first derivative of (3.17) in terms of x as

$$\begin{aligned}
\frac{d}{dx}\Big[{}_{-1}\mathcal{D}_x^{\sigma} u_N(x)\Big] &= \sum_{j=2}^{N} u_N(x_j) a_j \sum_{n=1}^{N} \beta_n^j \sum_{q=\lceil \sigma-\mu \rceil}^{n-1} b_{nq} \frac{d}{dx}\Big[(x+1)^{q+\mu-\sigma}\Big], \\
&= \sum_{j=2}^{N} u_N(x_j) \left[a_j \sum_{n=1}^{N} \beta_n^j \sum_{q=\lceil \sigma-\mu \rceil}^{n-1} b_{nq}^{*} (x+1)^{q+\mu-\sigma-1}\right],
\end{aligned}$$

where by evaluating the above expression at the collocation points, we obtain

$$\begin{aligned}
{}_{-1}\mathcal{D}_x^{1+\sigma} u_N(x)\Big|_{x=x_i} &= \sum_{j=2}^{N} u_N(x_j) \left[a_j \sum_{n=1}^{N} \beta_n^j \sum_{q=\lceil \sigma-\mu \rceil}^{n-1} b_{nq}^{*} (x_i+1)^{q+\mu-\sigma-1}\right], \\
&= \sum_{j=2}^{N} \mathbf{D}_{ij}^{1+\sigma} u_N(x_j),
\end{aligned} \tag{3.23}$$

in which $\mathbf{D}_{ij}^{1+\sigma}$ are the entries of $\mathbf{D}^{1+\sigma}$, computed as

$$\mathbf{D}_{ij}^{1+\sigma} = \frac{1}{(x_j+1)^{\mu}} \left[\sum_{n=1}^{N} \beta_n^j \sum_{q=\lceil \sigma-\mu \rceil}^{n-1} b_{nq}^{*} \, (x_i+1)^{q+\mu-\sigma-1} \right], \tag{3.24}$$

where $b_{nq}^{*} = (q+\mu-\sigma) b_{nq}$; see (3.18).

Remark 2. We note that the coefficients β_n^j, shown in (3.10), are obtained only *once* and are utilized as many as times needed to calculate $\mathbf{D}^{\sigma}$ or $\mathbf{D}^{1+\sigma}$ of any order $\sigma \in (0,1)$.

3.3. Collocation/interpolation points. In principle, the collocation and interpolation points can be chosen arbitrarily. However, the right choice of the collocation/interpolation points is the key to obtaining efficient schemes resulting in well-conditioned linear systems. Here, we examine five methods which yield different sets of collocation/interpolation points for the construction of the differentiation matrix $\mathbf{D}^{\sigma_1}$, and $\mathbf{D}^{1+\sigma_2}$, $\sigma_1, \sigma_2 \in (0,1)$. For general FODEs/FPDEs, where both $\mathbf{D}^{\sigma_1}$ and $\mathbf{D}^{1+\sigma_2}$ may appear, we consider N collocation points of *Gauss–Lobatto* type in order to include both boundary points. We refer to the aforementioned points as follows:

(i) *Equidistant points*: this choice is inspired by the well-known *Fourier* collocation points, and we obtain the N points as $x_i = -1 + \frac{2(i-1)}{N-1}$, $i = 1, 2, \ldots, N$.

(ii) *Roots of* ${}^{(1)}\widetilde{\mathcal{P}}_M^{\mu}(x) = (1+x)^{\mu} P_{M-1}^{-\mu,\mu}(x)$: the M zeros of such Jacobi polyfractonomial are essentially *Gauss–Radau* points, obtained through finding the $(M-1)$ roots of the Jacobi polynomial $P_{M-1}^{-\mu,\mu}(x)$ in addition to the left boundary point $x=-1$ due to the fractional multiplier term. Setting $M = N-1$ and including the right boundary point $x=1$ provides the N collocation/interpolation points needed.

(iii) *Roots of* ${}_{-1}\mathcal{D}_x^{\mu}[\, {}^{(1)}\mathcal{P}_M^{\mu}(x)\,]$: the corresponding $M-1$ roots are *Gauss* points, which lie in the interior domain in this case. Here, we can think of these collocation/interpolation points as the (fractional) *extrema* of the Jacobi polyfractonomial ${}^{(1)}\mathcal{P}_M^{\mu}(x)$ because we compute the roots of the (fractional) derivative of the eigenfunction. We perform such root finding easily using the property (3.4) and equivalently obtaining the $M-1$ roots of *Legendre* polynomial $P_{M-1}(x)$. Finally, we set $M = N-2$ and add both the left and right boundary points $x=-1$ and $x=1$ to provide the N points needed.

(iv) *Chebyshev roots,* $-\cos(\frac{(2j+1)}{M}\frac{\pi}{2})$, $j = 0, 1, \ldots, M-1$: the M roots of the Chebyshev polynomial $T_M(x)$ are also *Gauss* points. Hence, we set $M = N-2$ and similarly add both the left and right boundary points $x=-1$ and $x=1$.

(v) *Roots of* $dT_{N+1}(x)/dx$, *i.e.,* $-\cos(\frac{j\pi}{N-1})$, $j = 0, 1, \ldots, N-1$: this choice provides the N collocation/interpolation points which are the *extrema* points of the Chebyshev polynomial $T_{N+1}(x)$ roots. These N points are essentially of *Gauss–Lobatto* type and the boundary points $x = \pm 1$ are included automatically.

In order to examine the efficiency of each choice of collocation/interpolation points, we consider two canonical steady-state problems, namely, the one-dimensional steady-state space-fractional advection equation and the one-dimensional steady-state space-fractional diffusion problem. In these test cases, we compare the obtained accuracy in addition to the condition number of the corresponding linear system for the five aforementioned choices of the collocation/interpolation points.

3.3.1. Steady-state fractional advection equation. First, we consider the simplest FODE, the following space-fractional advection equation of order $\nu \in (0,1)$:

$$
\begin{aligned}
{}_{-1}\mathcal{D}_x^{\nu} u(x) &= f(x), \quad x \in [-1,1], \\
u(-1) &= 0.
\end{aligned}
\tag{3.25}
$$

We seek the solution to (3.25) in the form $u_N(x) = \sum_{j=2}^{N} u_N(x_j)\, h_j^{\mu}(x)$ (note that $u_N(x_1) = u_N(-1) = 0$). Then, by adopting one the collocation/interpolation points presented in section 3.3, and requiring the residual

$$
R_N^{adv}(x) = {}_{-1}\mathcal{D}_x^{\nu} u(x) - f(x) \tag{3.26}
$$

to vanish on the collocation points, and finally setting $\nu = \mu$, we obtain

$$
\sum_{j=2}^{N} \mathbf{D}_{ij}^{\mu}\; u_N(x_j) - f(x_i) = 0 \tag{3.27}
$$

for $i = 2, 3, \ldots, N$. Hence, the collocation scheme leads to the following linear system:

$$
\mathbf{D}^{\mu} \vec{\mathbf{u}_N} = \vec{\mathbf{f}}, \tag{3.28}
$$

in which $\mathbf{D}^{\mu}$ is the corresponding $(N-1) \times (N-1)$ fractional differentiation matrix given in (3.14).

Corresponding to the force-term $f(x) = \frac{\Gamma(7+9/17)}{\Gamma(7+9/17-\nu)}\ (1+x)^{6+9/17-\nu}$, the analytical solution to (3.25) is obtained as $u^{ext}(x) = (1+x)^{6+9/17}$, which is a fractional-order function. Having such an exact solution, we show the log-linear L^{∞}-norm error of the numerical solution to (3.25), versus N, in Figure 3.1. On the left side of the figure, we employ different collocation/interpolation points, and we present the corresponding condition number of the linear system resulting from each choice of collocation/interpolation points on the right side. We also examine three fractional orders, where the first row is associated with the fractional order $\nu = \mu = 1/10$, the middle row corresponds to $\nu = \mu = 1/2$, and the bottom row corresponds to $\nu = \mu = 9/10$. We first observe that our fractional collocation method yields exponential convergence (decay of the L^{∞}-error with N) in each case. We also observe that the roots of ${}_{-1}\mathcal{D}_x^{\nu}[\ {}^{(1)}\mathcal{P}_M^{\nu}(x)\ ]$, denoted as (fractional) extrema of the Jacobi polyfractonomials, are the best points among all cases. It is shown that not only does this choice lead to the best accuracy (lowest error level), but also it results in the lowest condition number with the slowest growth with respect to N.

3.3.2. Steady-state fractional diffusion problem. Next, we examine a higher-order FODE that is a space-fractional diffusion equation of order $1+\nu$, $\nu \in (0,1)$,

$$
\begin{aligned}
{}_{-1}\mathcal{D}_x^{1+\nu} u(x) &= f(x), \quad x \in [-1,1], \\
u(\pm 1) &= 0,
\end{aligned}
\tag{3.29}
$$

to analyze the performance of the higher differentiation matrices. We seek solutions to (3.29) in the form $u_N(x) = \sum_{j=2}^{N-1} u_N(x_j)\, h_j^{\mu}(x)$, where $u_N(x_1) = u_N(-1) = u_N(x_N) = u_N(+1) = 0$. Similarly, by requiring the residual to vanish on any choice of the collocation points given in section 3.3 and setting $\mu = \nu$, we obtain

$$
\sum_{j=2}^{N} \mathbf{D}_{ij}^{1+\mu}\; u_N(x_j) - f(x_i) = 0 \tag{3.30}
$$

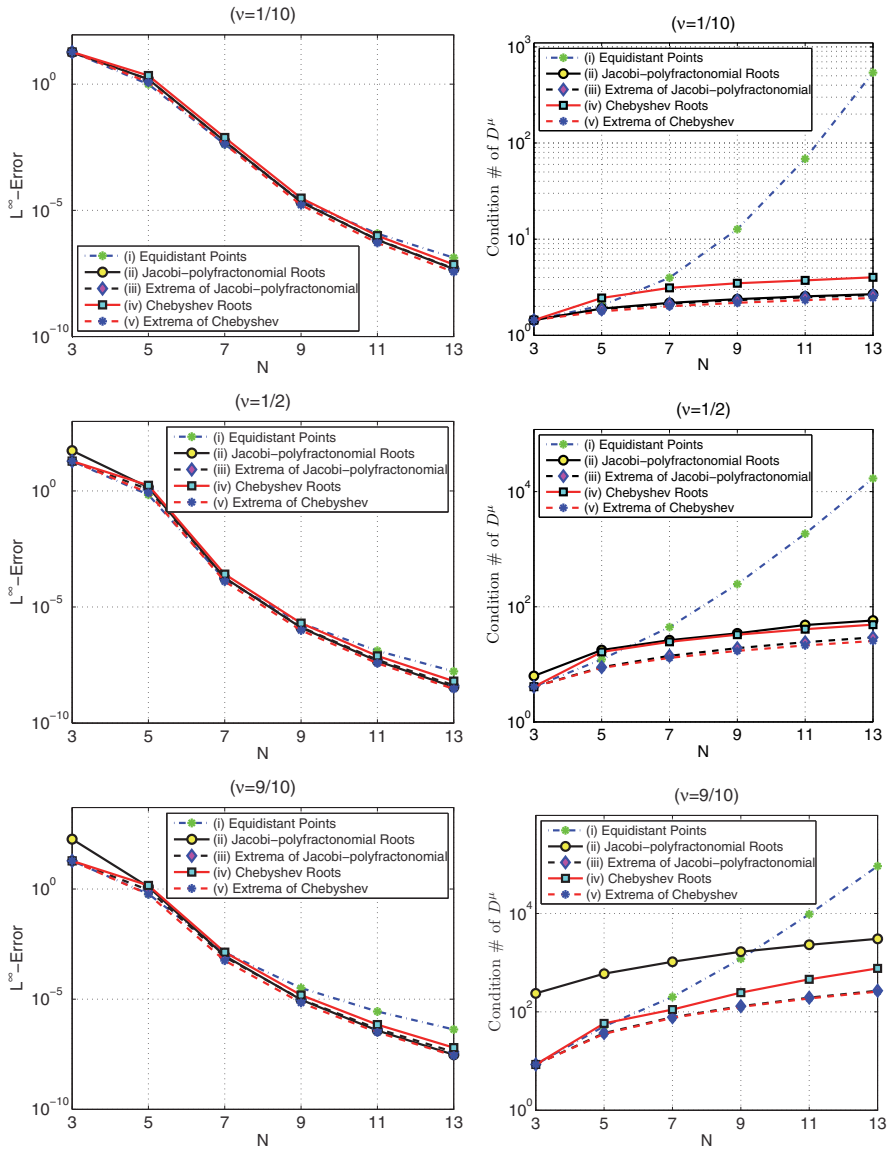

FIG. 3.1. *Steady-state fractional advection problem: log-linear L^∞-norm error of the numerical solution to ${}_{-1}\mathcal{D}_x^{\nu} u(x) = f(x)$, $x \in [-1,1]$, versus N, employing different collocation/interpolation points (left column), and the corresponding condition number of the linear system resulting from each choice of collocation/interpolation points (right column). The first row is associated with the fractional order $\nu = \mu = 1/10$, the middle row corresponds to $\nu = \mu = 1/2$, and the bottom row corresponds to the fractional order $\nu = \mu = 9/10$.*

for $i = 2, 3, \ldots, N-1$, which leads to the linear system

$$\mathbf{D}^{1+\mu}\vec{\mathbf{u}_N} = \vec{\mathbf{f}}, \tag{3.31}$$

in which $\mathbf{D}^{1+\mu}$ is the corresponding $(N-2)\times(N-2)$ fractional differentiation matrix given in (3.22). Having the same analytical solution taken in the previous case and in a similar fashion, we present the log-linear L^∞-norm error of the numerical solution

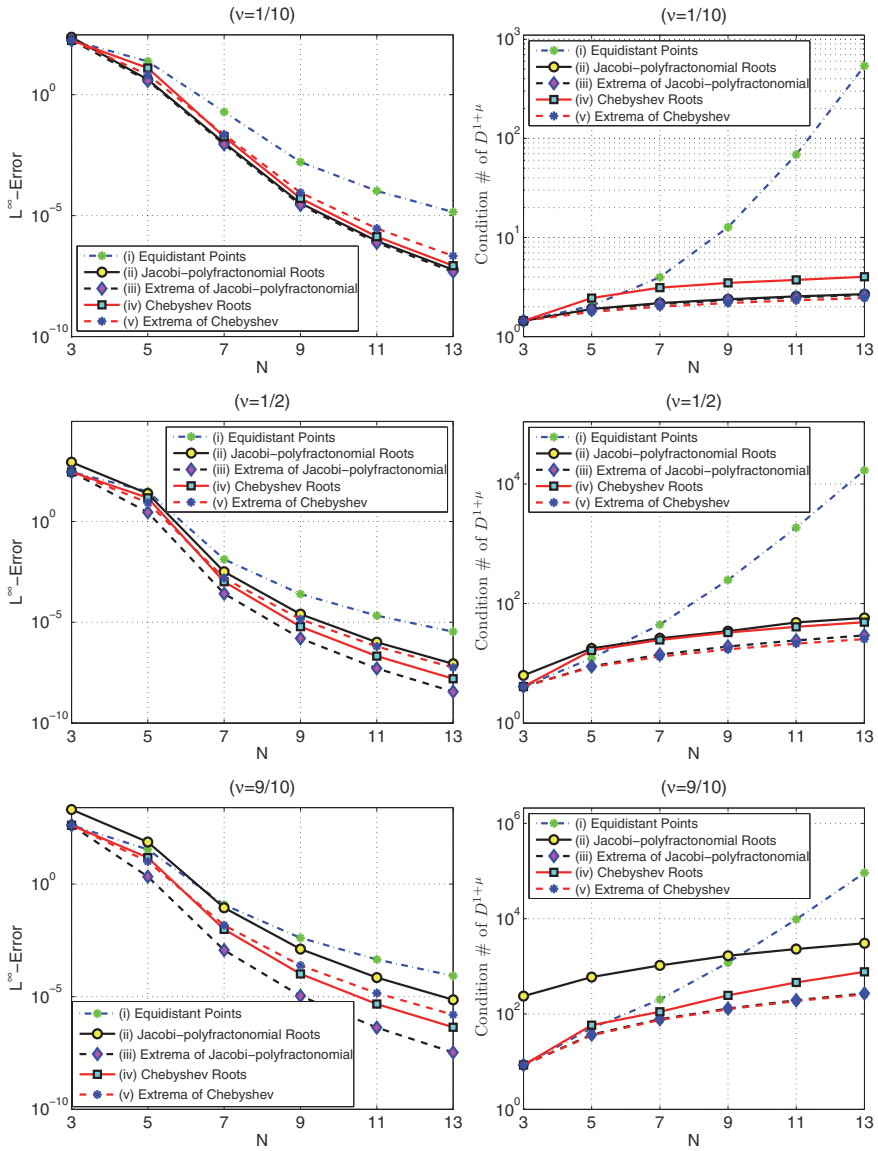

FIG. 3.2. *Steady-state fractional diffusion problem: log-linear L^∞-norm error of the numerical solution to ${}_{-1}\mathcal{D}_x^{1+\nu} u(x) = f(x)$, $x \in [-1,1]$, versus N, employing different collocation/interpolation points (left column), and the corresponding condition number of the linear system resulting from each choice of collocation/interpolation points (right column). The first row is associated with the fractional order $\nu = \mu = 1/10$ (of total order 1.1), the middle row corresponds to $\nu = \mu = 1/2$ (of total order 1.5), and the bottom row corresponds to the fractional order $\nu = \mu = 9/10$ (of total order 1.9).*

to ${}_{-1}\mathcal{D}_x^{1+\nu} u(x) = f(x)$, versus N, in Figure 3.2 on the left side, where different collocation/interpolation points are utilized. We also show the corresponding condition number of the linear system resulting from each choice on the right side. This numerical experiment is in agreement with our previous observation, which again highlights that the roots of ${}_{-1}\mathcal{D}_x^{\nu}[\,{}^{(1)}\mathcal{P}_M^{\nu}(x)\,]$, denoted as (fractional) extrema of the Jacobi polyfractonomials, are the best points.

4. Numerical tests. Having established the best choice of the collocation points in the previous section, we now present further numerical test cases. In fact, many applications might involve fractional differential operators consisting of multiple fractional derivative terms possibly with different fractional order. In this section, we solve a number of linear and nonlinear FPDEs to investigate the performance of our fractional collocation method.

4.1. Steady-state problems. We first examine two linear steady-state problems: (i) the space-fractional advection-diffusion equation and (ii) space-fractional multi-term FODEs. Here, we take a step-by-step approach to show how the FSCM can be employed to solve different problems with almost the same ease.

4.1.1. Steady-state fractional advection-diffusion. Here, we consider a two-term equation that describes the dynamics of the steady-state fractional advection-diffusion problem. Particularly, we are interested in the following case:

$$c\ {}_{-1}\mathcal{D}_x^{\nu_1} u(x) - K\ {}_{-1}\mathcal{D}_x^{1+\nu_2} u(x) = f(x), \quad x \in [-1,1], \qquad u(\pm 1) = 0, \tag{4.1}$$

where ν_1 and $\nu_2 \in (0,1)$.

Remark 3. Problem (3.25) was associated only with a single fractional order ν, for which we could perform the interpolation (3.7). However, in (4.1), the fractional differential operator generally is associated with two fractional orders. Hence, we need to specify a *representative fractional order*, ν_{rep}, to do interpolation operation at the collocation points. Such ν_{rep} can be simply set as the average of the fractional orders in (4.1) or as the max/min$\{\nu_1, \nu_2\}$.

This time, we seek the solution to (4.1) as $u_N(x) = \sum_{j=2}^{N-1} u_N(x_j)\, h_j^{\mu}(x)$ considering $\mu = \nu_{rep}$, where due to the homogeneous boundary conditions, $u_N(x_1) = u_N(-1) = 0 = u_N(1) = u_N(x_N)$, we construct $h_j^{\mu}(x)$ only for $j = 2, 3, \ldots, N-1$. Then, by requiring the corresponding residual to vanish at the collocation points $\{x_i\}_{i=2}^{N-1}$,

$$c \sum_{j=2}^{N-1} \mathbf{D}_{ij}^{\nu_1}\ u_N(x_j)\ - K \sum_{j=2}^{N-1} \mathbf{D}_{ij}^{1+\nu_2}\ u_N(x_j) - f(x_i) = 0, \tag{4.2}$$

we obtain the linear system

$$\mathbf{D}_{tot}^{\nu} \vec{\mathbf{u}}_N = \vec{\mathbf{f}}, \tag{4.3}$$

where $\mathbf{D}_{tot}^{\nu} = c\mathbf{D}^{\nu_1} - K\mathbf{D}^{1+\nu_2}$ of dimension $(N-2) \times (N-2)$, in which $\mathbf{D}^{1+\nu_2}$ is obtained from (3.22) or (3.24).

To demonstrate the performance of the collocation scheme for such an application, we consider the forcing term

$$f(x) = \frac{\Gamma(\frac{128}{17})}{\Gamma(\frac{128}{17} - \nu_1)}\ (1+x)^{\frac{111}{17} - \nu_1} - \left(\frac{111}{17} - \nu_2\right) \frac{\Gamma(\frac{128}{17})}{\Gamma(\frac{128}{17} - \nu_2)}\ (1+x)^{\frac{94}{17} - \nu_2}, \tag{4.4}$$

for which the analytical solution to (4.1) is obtained as $u^{ext}(x) = (1+x)^{6+9/17}$. In Figure 4.1, we show the log-linear L^{∞}-norm error of the numerical solution to ${}_{-1}\mathcal{D}_x^{\nu_1} u(x) - {}_{-1}\mathcal{D}_x^{1+\nu_2} u(x) = f(x)$, $x \in [-1,1]$, versus N, employing different fractional orders ν_1 and ν_2 (left column) and the corresponding condition number of

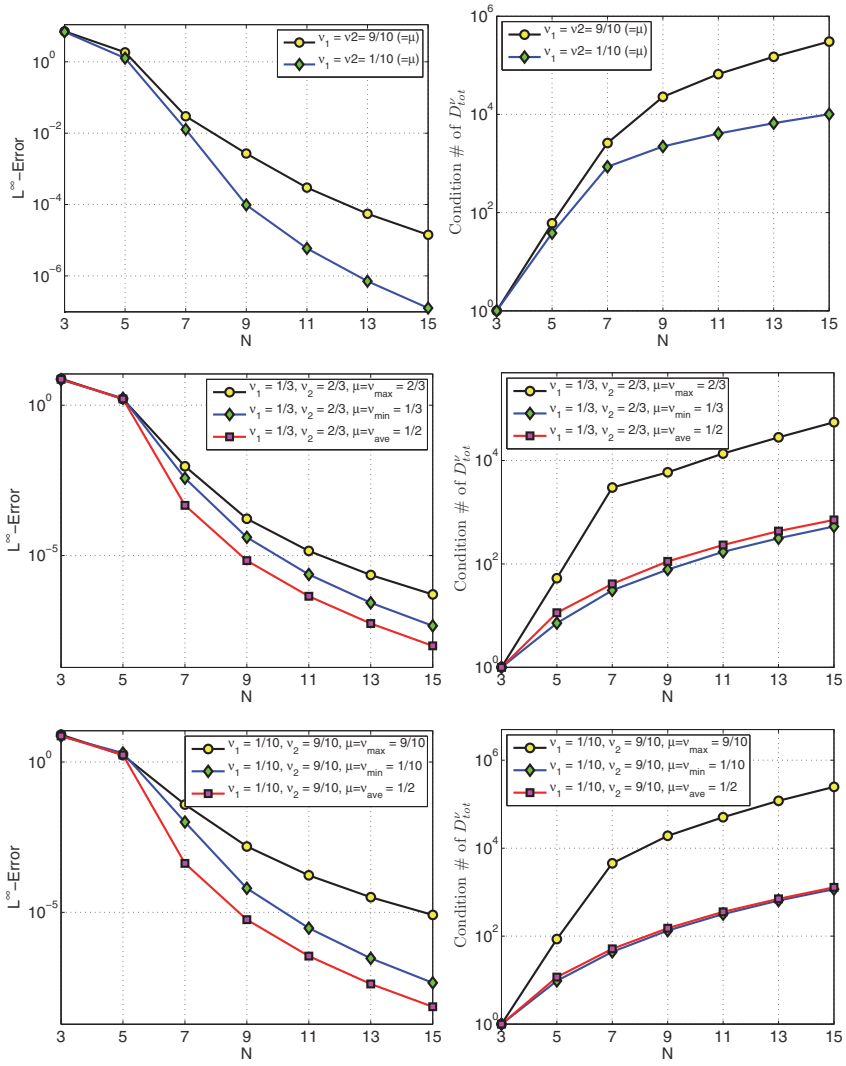

FIG. 4.1. *Steady-state fractional advection-diffusion: log-linear L^∞-norm error of the numerical solution to $c\ {}_{-1}\mathcal{D}_x^{\nu_1} u(x) - K\ {}_{-1}\mathcal{D}_x^{1+\nu_2} u(x) = f(x)$, $x \in [-1,1]$, versus N, employing different fractional orders ν_1 and ν_2 (left column), and the corresponding condition number of the linear system resulting form each choice of fractional order (right column).*

the linear system resulting form each choice of fractional order (right column). In this figure, the first row is associated with the fractional order $\nu_1 = \nu_2 = \mu$, and the middle row corresponds to the case where $\nu_1 < \nu_2$ where the fractional interpolation parameter μ is taken as ν_{max}, ν_{min}, and ν_{ave}; similarly, the bottom row corresponds to $\nu_1 < \nu_2$ such that for this case $\nu_2 - \nu_1$ becomes larger than that considered in the middle row.

The exponential decay of the L^∞-norm error with N is the first observation we make in Figure 4.1. Here we employ the roots of ${}_{-1}\mathcal{D}_x^{\nu}[\ {}^{(1)}\mathcal{P}_M^{\nu}(x)\ ]$, (fractional) extrema of the Jacobi polyfractonomials, as our collocation/interpolation points. The second important observation is about the choice of the fractional interpolation parameter μ, since we have two different fractional orders, ν_1 and ν_2. It was shown that

among $\mu = \nu_{max}$, ν_{max}, and ν_{ave}, the average value, i.e., $\mu = \nu_{ave}$, shows the fastest decay of error with N in Figure 4.1 in addition to yielding almost the slowest growth of the condition number with N in the corresponding linear system.

4.1.2. Multiterm linear advection-diffusion-reaction equations. Next, we generalize (3.25) to a multiterm linear fractional differential equation as

$$\sum_{k=1}^{M_a} c_k \Big[{}_{-1}\mathcal{D}_x^{\nu_k} u(x) \Big] + \sum_{p=1}^{M_d} \mathcal{C}_k \Big[{}_{-1}\mathcal{D}_x^{1+\sigma_p} u(x) \Big] + \mathfrak{M}\, u(x) = f(x),\ x \in [-1,1], \tag{4.5}$$
$$u(\pm 1) = 0,$$

where $\mathcal{C}_{M_d} \neq 0$, ν_k, and $\sigma_p \in (0,1)$; moreover, $\{c_k\}_{k=1}^{M_a}$, $\{\mathcal{C}_p\}_{p=1}^{M_d}$ also $\mathfrak{M}$ are real constants given.

We follow similar steps and seek the solution to (4.5) as $u_N(x) = \sum_{j=2}^{N-1} u_N(x_j)\, h_j^{\mu}(x)$ by setting μ to some representative ν. Next, by requiring the corresponding residual to vanish at the collocation points $\{x_i\}_{i=2}^{N-1}$ (the roots of the Jacobi polyfractonomial), we obtain

$$\sum_{k=1}^{M_a} c_k \Big[{}_{-1}\mathcal{D}_x^{\nu_k} u(x) \Big]_{x=x_i} + \sum_{p=1}^{M_d} \mathcal{C}_k \Big[{}_{-1}\mathcal{D}_x^{1+\sigma_p} u(x) \Big]_{x=x_i} + \mathfrak{M}\, u(x_i) - f(x_i) = 0,$$

where the fractional differentiation matrices $\mathbf{D}^{\nu_k}$, $k = 1, 2, \ldots, M_a$, and $\mathbf{D}^{1+\sigma_p}$, $p = 1, 2, \ldots, M_d$, are obtained form (3.20) and (3.24). By doing so, the collocated fractional differential equation results in the linear (algebraic) system

$$\mathbf{D}_{tot}^{\nu,\sigma}\ \vec{\mathbf{u}}_N = \vec{\mathbf{f}}, \tag{4.6}$$

where $\mathbf{D}_{tot}^{\nu,\sigma} = \sum_{k=1}^{M_a} \mathbf{D}^{\nu_k} + \sum_{p=1}^{M_d} \mathbf{D}^{1+\sigma_p} + \mathfrak{M}\, I$ represents the total fractional differentiation matrix whose dimension is $(N-2)\times(N-2)$, in which I denotes the identity matrix.

In Figure 4.2, left, we plot the log-linear L^∞-norm error of the numerical solution to (4.5), versus N, corresponding to different fractional orders ν_k and σ_p. In this case, we take the exact solution to be $u^{ext}(x) = (1+x)^{6+9/17} - 2(1+x)^{5+9/17}$. These results once again confirm the exponential convergence of the fractional collocation method and verify that the choice of fractional interpolation parameter μ as the *algebraic mean* of all fractional differential orders leads to the fastest exponential convergence. The corresponding condition number obtained for such average value, μ, also leads to small growth with respect to N (see the right side of Figure 4.2).

4.2. Time-dependent FPDEs. We examine time-dependent FPDEs in which both spatial and temporal differential terms are considered as fractional order. Specifically, we consider time- and space-fractional advection-diffusion equation, time- and space-fractional multiterm FPDEs, and finally the time-dependent space-fractional nonlinear Burgers equation.

4.2.1. Time- and space-fractional advection-diffusion. As the first time-dependent FPDE, we consider the following problem:

$${}_0\mathcal{D}_t^{\tau} u(x,t) + c\, {}_{-1}\mathcal{D}_x^{\nu_1} u(x,t) - K\, {}_{-1}\mathcal{D}_x^{1+\nu_2} u(x,t) = f(x,t), \quad x \in [-1,1],\ t \in [0,T], \tag{4.7}$$
$$u(\pm 1, t) = 0,$$
$$u(x,0) = 0,$$

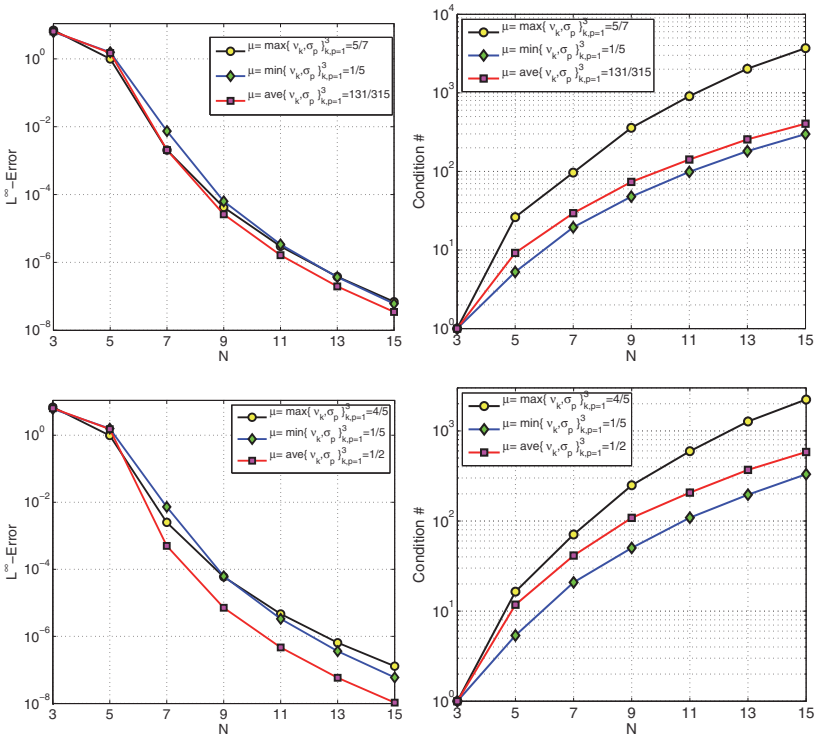

FIG. 4.2. *Steady-state multiterm problem: log-linear L^∞-norm error of the numerical solution to* (4.5)*, versus N, employing fractional orders (left column), and the corresponding condition number of the linear system resulting form each choice of fractional order (right column). Top row corresponds to the fractional orders $\nu_1 = \sigma_1 = 1/5$, $\nu_2 = \sigma_2 = 1/3$, and $\nu_3 = \sigma_3 = 5/7$, and bottom row corresponds to $\nu_k = 1 - \sigma_k$, where $\sigma_1 = 1/5$, $\sigma_2 = 1/3$, $\sigma_3 = 5/7$.*

where $x \in [-1, 1]$ and $t \in [0, T]$, and the associated fractional orders are τ, ν_1, and $\nu_2 \in (0, 1)$. We seek the solution of the form

$$u_N^M(x,t) = \sum_{j=1}^{N} \sum_{m=1}^{M} u_N^M(x_j, t_m) h_j^{\mu_x}(x) l_m^{\mu_t}(t), \tag{4.8}$$

where $h_j^{\mu_x}(x)$ are the spatial fractional Lagrange basis functions with the representative fractional parameter μ_x, and $l_m^{\mu_t}(t)$ represent the corresponding temporal nodal basis functions with the representative parameter μ_t, constructed as

$$l_m^{\mu_t}(t) = \Big(\frac{t}{t_m}\Big)^{\mu_t} \prod_{\substack{q=1 \\ q \neq m}}^{M} \Big(\frac{t - t_q}{t_m - t_q}\Big), \quad 2 \leq q \leq M, \tag{4.9}$$

where the collocation points can be taken as $t_i = (x_i + 1)T/2$, where x_i are the spatial collocation points, such that $0 = t_1 < t_2 < \cdots < t_N = T$. By taking similar steps as in section 3.1 and setting $\tau = \mu_t$, we can obtain the time-fractional differentiation matrix $\mathbf{D}^{\mu_t}$, whose entries are given as

$$\mathbf{D}_{ij}^{\mu_t} = \frac{1}{(t_m)^{\mu_t}} \sum_{m=1}^{M} \frac{\Gamma(m + \mu_t)}{\Gamma(m)} \beta_n^j P_{n-1}(x(t_i)). \tag{4.10}$$

Such temporal fractional interpolants satisfy the property $l_m^{\mu_t}(x_k) = \delta_{mk}$ at the time interpolation points. We note that the same β_n^j utilized for the space-fractional differentiation matrix are employed in (4.10). Next, we substitute (4.8) into (4.7) and take the interpolation and collocation points to be identical. Then, by the Kronecker property for both time- and space-fractional Lagrange interpolants we obtain

$$\mathbf{U}\mathbf{D}^{\mu_t\,T} + [c\,\mathbf{D}^{\nu_1} - K\,\mathbf{D}^{1+\nu_2}]\,\mathbf{U} = \mathbf{F}, \tag{4.11}$$

in which $\mathbf{U}$ and $\mathbf{F}$ denote the matrix of approximate solution and load matrix whose entries are $u_N^M(x_j, t_m)$ and $f(x_j, t_m)$, respectively. The linear system (4.11) can be viewed as a *Lyapunov* equation

$$\mathbf{A}\,\mathbf{U} + \mathbf{U}\mathbf{B} = \mathbf{F}, \tag{4.12}$$

where $\mathbf{A} = c\,\mathbf{D}^{\nu_1} - K\,\mathbf{D}^{1+\nu_2}$ and $\mathbf{B} = \mathbf{D}^{\mu_t\,T}$. Here, the superscript ^{T} represents the transpose operation.

Since we have already studied the spatial discretization of our scheme, the temporal accuracy is now examined in Figure 4.3, where the aim is to show the exponential decay of the time-integration error with N, for which the exact solution is taken as $u^{ext}(x,t) = t^{6+2/3}\left((1+x)^{6+9/17} - 2(1+x)^{5+9/17}\right)$. We employ the fractional extrema of the Jacobi polyfractonomial as the time interpolation points and plot the log-linear L^∞-norm error of the numerical solution to (4.7), versus M, corresponding to advection fractional order $\nu_1 = 1/3$ and $\nu_2 = 2/3$, i.e., total diffusive order $1 + 2/3$ (left) and $\nu_1 = 1/10$ and $\nu_2 = 9/10$ (right). In each case shown in Figure 4.3, we examine the time-fractional orders $\tau = 1/10$ and $9/10$.

4.2.2. Time- and space-fractional multiterm FPDEs. Next, we generalize the fractional advection-diffusion problem (4.7) to a multiterm linear FPDE as

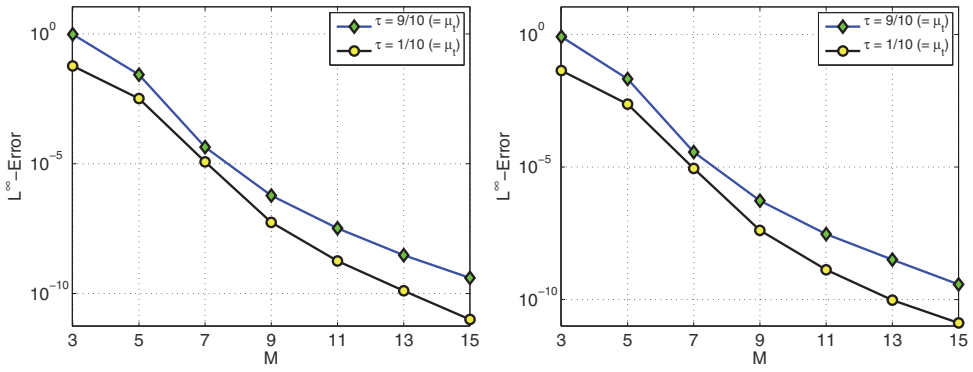

FIG. 4.3. *Time- and space- fractional advection-diffusion problem; log-linear L^∞-norm error of the numerical solution to* 4.7*, versus M, corresponding to advective fractional order $\nu_1 = 1/3$ and $\nu_2 = 2/3$, i.e., total diffusive order $1 + 2/3$ (left), and $\nu_1 = 1/10$ and $\nu_2 = 9/10$ (right). In each case, we examine the time-fractional orders $\tau = 1/10$ and $9/10$, where the time integration is performed for simulation time $T = 1$. Here, the left panel corresponds to the space-fractional orders $\nu_1 = 1/3$ and $\nu_2 = 2/3$, while the right panel corresponds to $\nu_1 = 1/10$ and $\nu_2 = 9/10$.*

(4.13)
$$
\begin{aligned}
&{}_0\mathcal{D}_t^{\tau} u(x,t) + \sum_{k=1}^{M_a} c_k \Big[{}_{-1}\mathcal{D}_x^{\nu_k} u(x,t) \Big] \\
&\quad + \sum_{p=1}^{M_d} \mathcal{C}_k \Big[{}_{-1}\mathcal{D}_x^{1+\sigma_p} u(x,t) \Big] + \mathfrak{M}\, u(x,t) = f(x,t), \quad x \in [-1,1],\ t \in [0,T], \\
&\qquad\qquad u(\pm 1, t) = 0, \\
&\qquad\qquad u(x,0) = 0,
\end{aligned}
$$

where $\mathcal{C}_{M_d} \neq 0$, τ, ν_k, and $\sigma_p \in (0,1)$. In addition, $\{c_k\}_{k=1}^{M_a}$, $\{\mathcal{C}_p\}_{p=1}^{M_d}$, and $\mathfrak{M}$ are real constants given as before. Taking similar steps as in section 4.2.1 leads to another Lyapunov matrix equation

$$
\widetilde{\mathbf{A}}\,\mathbf{U} + \mathbf{U}\widetilde{\mathbf{B}} = \mathbf{F}, \tag{4.14}
$$

in which $\widetilde{\mathbf{A}} = \sum_{k=1}^{M_a} c_k \mathbf{D}^{\nu_k} + \sum_{p=1}^{M_d} \mathcal{C}_k \mathbf{D}^{1+\nu_p}$ and $\widetilde{\mathbf{B}} = \mathbf{B} = \mathbf{D}^{\mu_t T}$.

We confirm our observation made in the previous case in Figure 4.4, where we plot the log-linear L^∞-norm error of the numerical solution to (4.13), versus N. On the left side of the figure the distributed advective fractional orders are taken as $\nu_k = 1 - \sigma_k$, $k = 1, 2, 3$, where $\sigma_1 = 1/5$, $\sigma_2 = 1/3$, and $\sigma_3 = 5/7$. On the right side of the figure, the associated fractional orders are $\nu_k = \sigma_k$. In each case, we examine time-fractional orders $\tau = 1/10$ and $9/10$. We have taken the same exact solution as in the previous case, however with a different corresponding forcing term $f(x,t)$, obtained using (2.8). We similarly observed that the algebraic mean of the fractional differentiation orders would be an appropriate candidate for μ, the fractional interpolation parameter.

4.2.3. Time-dependent space-fractional Burgers equation. We shall show one of the most important advantages of our fractional collocation method that is the

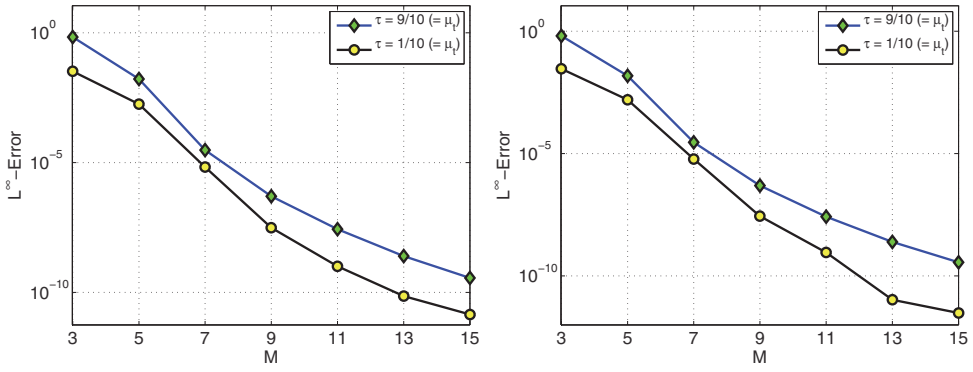

FIG. 4.4. *Time-and space-fractional multiterm problem; log-linear L^∞-norm error of the numerical solution to* 4.13*, versus M, where the exact solution $u^{ext}(x,t) = t^{6+2/3}\,(\,(1+x)^{6+9/17} - 2(1+x)^{5+9/17}\,)$. The temporal fractional derivative order is τ, the multiterm advective fractional orders are shown by ν_k,$k = 1,2,3$, and the diffusive fractional orders are denoted by $1+\sigma_k$. The left figure corresponds to multiterm advective fractional orders $\nu_k = 1-\sigma_k$, $k = 1,2,3$, where $\sigma_1 = 1/5$, $\sigma_2 = 1/3$,and $\sigma_3 = 5/7$. The right figure is associated with the $\nu_k = \sigma_k$. In each case, we examine time-fractional orders $\tau = 1/10$ and $9/10$, where the time integration is performed for simulation time $T = 1$.*

efficient treatment of the nonlinear fractional differential terms in FPDEs. As for the last problem, we solve the time-dependent space-fractional Burgers equation

(4.15)
$$\frac{\partial u}{\partial t} + u(x,t)\ {}_{-1}\mathcal{D}_x^{\nu_1} u(x,t) - \epsilon\ {}_{-1}\mathcal{D}_x^{1+\nu_2} u(x,t) = f(x,t), \quad x \in [-1,1],\ t \in [0,T],$$
$$u(\pm 1, t) = 0,$$
$$u(x,0) = 0,$$

where ν_1 and $\nu_2 \in (0,1)$. The corresponding spatial discretization can be done in a similar fashion as shown in previous sections as

$$\frac{d\vec{\mathbf{u}_N}(t)}{dt} = -\mathrm{diag}[\,\vec{\mathbf{u}_N}(t)\,]\mathbf{D}^{\nu_1}\vec{\mathbf{u}_N}(t) + \epsilon\ \mathbf{D}^{1+\nu_2}\vec{\mathbf{u}_N}(t) + \vec{\mathbf{f}}(t), \tag{4.16}$$

where $\mathrm{diag}[\,\vec{\mathbf{u}_N}(t)\,]$ represents a diagonal matrix whose diagonal entries are the components of the solution vector $\vec{\mathbf{u}_N}(t)$. The time integration of this system can be done using a fourth-order Runge–Kutta (RK-4). In Table 4.1 we show the exponential decay of L^∞-norm error of the numerical solution to (4.15) with N, corresponding to the fractional orders $\nu_1 = \nu_2 = 1/2$, and the simulation time $T = 1/2$. In our RK-4 multistage time-integration scheme, we utilize $\Delta t = 5\times 10^{-6}$. We have examined three values for ϵ: (i) $\epsilon = 0$ corresponding to the inviscid Burgers equation, (ii) $\epsilon = 10^{-4}$ corresponding to the viscous Burgers equation with comparatively small diffusivity, and (iii) $\epsilon = 10^{-3}$ corresponding to the viscous Burgers equation with comparatively larger diffusivity. Here, we set the exact solution $u^{ext}(x,t) = \exp(-t)\,(1-x)(1+x)^{5+9/17}$ for these test cases and obtain the corresponding forcing term for each case as

(4.17)
$$\begin{aligned} f(x,t) = &\sum_{q=1}^{\infty} \frac{(-1)^q \Gamma(q+1)}{(\Gamma+1-\tau)q!} t^{q-\tau} \\ &+ \exp(-t)\, u^{ext}(x,t) \Big[\frac{2p_0}{p_0-\nu_1}(1+x)^{p_0-1-\nu_1} - \frac{p_0+1}{p_0+1-\nu_1}(1+x)^{p_0-\nu_1}\Big] \\ &- \epsilon\ \exp(-t)\Big[\frac{2p_0(p_0-1-\nu_2)}{p_0-\nu_2}(1+x)^{p_0-2-\nu_2} \\ &- \frac{(p_0+1)(P_0-1-\nu_2)}{p_0+1-\nu_2}(1+x)^{p_0-1-\nu_2}\Big], \end{aligned}$$

where $p_0 = 6 + 9/17$, and we truncate the above infinite sum according to machine precision.

TABLE 4.1

Exponential decay of L^∞-norm error of the numerical solution to (4.15) with N, corresponding to the fractional orders $\nu_1 = \nu_2 = 1/2$, and the simulation time $T = 1/2$. In the RK-4 multistage time-integration scheme, we use $\Delta t = 5 \times 10^{-6}$.

N	Inviscid Burgers	Viscous Burgers ($\epsilon = 10^{-4}$)	Viscous Burgers ($\epsilon = 10^{-3}$)
3	1.8650958	1.8651994	1.8661323
5	0.5973899	0.6805485	0.6815204
7	2.03×10^{-4}	2.41×10^{-4}	2.43×10^{-4}
9	8.71×10^{-6}	8.68×10^{-6}	8.51×10^{-6}

5. Summary and discussion. In this study, we developed an exponentially accurate FSCM for solving steady-state and time-dependent FPDEs. First, we introduced *fractional Lagrange interpolants*, which satisfy the Kronecker delta property at collocation points. We performed such a construction following a spectral theory developed in [33] for FSLPs. Moreover, we obtained the corresponding fractional differentiation matrices and solved a number of linear and nonlinear FPDEs to investigate the numerical performance of the fractional collocation method. To this end, we introduced new candidate choices for collocation/interpolation points, namely, roots of Jacobi polyfractonomial ${}^{(1)}\mathcal{P}_M^{\mu}(x)$ and roots of ${}_{-1}\mathcal{D}_x^{\mu}[\,{}^{(1)}\mathcal{P}_M^{\mu}(x)\,]$, denoted as (fractional) *extrema* of the Jacobi polyfractonomial. We compared these new sets of residual-vanishing points with other existing standard interpolation/collocation points such as roots of Chebyshev polynomials, extrema of Chebyshev polynomials, and equidistant points. We numerically demonstrated that the roots of ${}_{-1}\mathcal{D}_x^{\mu}[\,{}^{(1)}\mathcal{P}_M^{\mu}(x)\,]$ are the best among others leading to minimal condition number in the corresponding linear system and fastest decay of L^{∞}-norm error.

We considered steady-state problems such as the space-fractional advection-diffusion problem and generalized space-fractional multiterm problems, as well as time-dependent FPDEs such as time- and space-fractional advection-diffusion equation, time- and space-fractional multiterm FPDEs, and finally the space-fractional Burgers equation. Our numerical results confirmed the exponential convergence of the fractional collocation method. We discuss the performance of FSCM in comparison with other approaches. In fact, among other high-order Galerkin spectral methods, and finite difference schemes developed for FPDEs, our FSCM scheme has a number of advantages, including (i) ease of implementation, (ii) lower computational cost, and (iii) exponential accuracy. In the following we elaborate on each of these features.

In terms of computational cost, the computational complexity of mathematical operations in the construction of $\mathbf{D}^{\sigma}$ and $\mathbf{D}^{1+\sigma}$ can be shown to be of $\mathcal{O}(N^2)$. Moreover, the computational cost of the presented method for steady-state linear FODEs can be shown to be associated mainly with (i) the construction of the differentiation matrices and (ii) the linear system solver. Then, the computational cost of the presented scheme is asymptotically $\mathcal{O}(\,(M_a + M_d)N^2 + N^3)$ for such FODEs, where M_a and M_d represent the number of advection- and diffusion-looking terms, respectively. For the time-dependent multiterm FPDEs presented, the cost of the scheme grows as $\mathcal{O}((M_a + M_d)N^2 + (MN)^3)$, when a direct solver is employed.

In contrast to the standard Galerkin projection schemes, there is no quadrature performed in our FSCM. Moreover, the treatment of nonlinear terms in FSCM can be done with the same ease as in linear problems. This is significant because solving nonlinear FPDEs remains a challenge in Galerkin methods. In addition, although the employment of Galerkin methods in linear FPDEs becomes conceptually similar to FSCM, Galerkin spectral methods with the traditional (polynomial) basis functions do not always lead to exponential convergence, as they do in our FSCM. Another important barrier in Galerkin projection schemes is the difficulty of treating multiterm FPDEs, where no straightforward variational form can be efficiently obtained for such problems. In contrast, we have clearly shown that our FSCM requires no extra effort to solve such multiterm FPDEs. Despite the aforementioned advantages of FSCM, the drawback of FSCM is that there is no rigorous theoretical framework for collocation schemes in general.

We conclude the paper by comparing the performance of FSCM with the FDM developed in [21], where the fractional derivative ${}_0\mathcal{D}_t^{\nu}u(t)$ is represented as

$$ {}_0\mathcal{D}_t^{\nu} u(t) = \frac{1}{\Gamma(2-\nu)} \sum_{j=0}^{k} b_j \frac{u(t_{k+1-j}) - u(t_{k-j})}{(\Delta t)^{\nu}} + r_{\Delta t}^{k+1}, \tag{5.1} $$

where $r_{\Delta t}^{k+1} \leq C_u (\Delta t)^{2-\nu}$ and $b_j := (j+1)^{1-\nu} - j^{1-\nu}, j = 0, 1, \ldots, k$; a central difference method has been employed to approximate the kernel in the fractional derivative. FDMs are usually easy schemes to implement; however, they are of low order of accuracy, which potentially leads to enormous memory storage in solving FPDEs when relatively well-resolved solutions are needed. Here, we solve the simplest fractional-order differential equation of the form

$$ \begin{aligned} {}_0\mathcal{D}_t^{\nu} u(\,t\,) &= f(t), \quad t \in [0, T], \\ u(0) &= 0, \end{aligned} \tag{5.2} $$

where ν is taken as $1/10$, $1/2$, and $9/10$, and the simulation time is set to $T = 1$. Such a model problem and the aforementioned FDM scheme are actually a building block for solving more complicated FPDEs, where the time- and space-fractional terms are discretized in a similar fashion. Moreover, in solving a multiterm FPDE with K fractional-order terms, one has to reformulate the problem into a recurrence system of fractional-order problems resembling (5.2) (see, e.g., [22]). However, as we have shown, our FSCM scheme solves any linear multiterm FPDE with the same ease and without resorting to reformulating the original problem.

To highlight this fact, we want to compare the CPU time in FSCM and the FDM scheme, in addition to a PG spectral method, developed in [34]. In this method, we seek an approximate solution of the form

$$ u(t) \approx u_N(t) = \sum_{n=1}^{N} a_n \, {}^{(1)}\widetilde{\mathcal{P}}_n^{\mu}(t), \tag{5.3} $$

where a_n are the unknown expansion coefficients to be determined. By plugging (5.3) into (5.2), we obtain the residual $R_N(t)$ as

$$ R_N(t) = {}_0\mathcal{D}_t^{\nu} u_N(t) - f(t) $$

to be L^2-orthogonal to all elements in the set of test functions $\{ {}^{(2)}\widetilde{\mathcal{P}}_k^{\mu}(\,x(t)\,) : \; k = 1, 2, \ldots, N\}$, which are the exact eigenfunctions of the FSLPs of the second kind [33]. This scheme yields a *diagonal* stiffness matrix, whose diagonal entries are given by $\gamma_k = (\frac{2}{T})^{2\mu-1} (\frac{\Gamma(k+\mu)}{\Gamma(k)})^2 \frac{2}{2k-1}$. Consequently, we obtain the expansion coefficients as

$$ a_k = \frac{1}{\gamma_k} \int_0^T f(t) \; {}^{(2)}\widetilde{\mathcal{P}}_k^{\mu}(\,x(t)\,)\, dt, \;\; k = 1, 2, \ldots, N. \tag{5.4} $$

In Table 5.1, we show the CPU time corresponding to FSCM, the PG spectral method, and FDM for solving (5.2) corresponding to the following three-level of L^{∞}-norm error: $\mathcal{O}(10^{-4})$, $\mathcal{O}(10^{-5})$, and $\mathcal{O}(10^{-6})$. Here, the exact solution is taken as $u^{ext}(t) = t^6$, where by setting $T = 1$, the computational cost of each method is shown corresponding to fractional order $\nu = 1/10$ (top), $\nu = 1/2$ (middle), and $\nu = 9/10$ (bottom). Table 5.1 reveals that for the whole range ν, and for the whole range of error level of interest, our FSCM and PG spectral method by far outperform FDM. Quantitatively, at the error level $\mathcal{O}(10^{-6})$, the FSCM and the PG method perform roughly 7 and 386 times faster than FDM corresponding to $\nu = 1/10$ and $\nu = 1/2$, respectively. However, we see that for such a simple model problem and setting,

TABLE 5.1

CPU time (seconds) on a single 2.66*-GHz Intel processor, corresponding to FSCM, the PG spectral method, and FDM for solving* ${}_0\mathcal{D}_t^\nu u(t) = f(t)$*, and the exact solution is* $u^{ext}(t) = t^6$*. Here,* N *denotes the expansion order in FSCM and the PG spectral method,* N_g *represents the number of grid points in FDM, and the simulation time is set to* $T = 1$*.*

		($\nu = 1/10$)	
L^∞-norm error	FSCM	PG spectral method	FDM
$\mathcal{O}(10^{-4})$	($N = 6$) 0.474261	($N = 6$) 0.519422	($N_g = 70$) 0.412937
$\mathcal{O}(10^{-5})$	($N = 7$) 0.54725	×	($N_g = 260$) 0.574912
$\mathcal{O}(10^{-6})$	($N = 8$) 0.726889	($N = 7$) 0.538418	($N_g = 1000$) 5.43267
		($\nu = 1/2$)	
L^∞-norm error	FSCM	PG spectral method	FDM
$\mathcal{O}(10^{-4})$	($N = 6$) 0.490258	($N = 6$) 0.494925	($N_g = 450$) 1.20882
$\mathcal{O}(10^{-5})$	($N = 7$) 0.551916	×	($N_g = 2000$) 21.9763
$\mathcal{O}(10^{-6})$	($N = 8$) 0.740887	($N = 7$) 0.501629	($N_g = 7000$) 285.797
		($\nu = 9/10$)	
L^∞-norm error	FSCM	PG spectral method	FDM
$\mathcal{O}(10^{-4})$	($N = 5$) 0.434934	×	($N_g = 3500$) 69.9344
$\mathcal{O}(10^{-5})$	($N = 6$) 0.497591	($N = 6$) 0.491425	($N_g = 26000$) 4714.55
$\mathcal{O}(10^{-6})$	($N = 7$) 0.531419	($N = 7$) 0.502424	Running out of memory!

FDM cannot achieve the error level $\mathcal{O}(10^{-6})$, because of the lack of memory. Instead, the FSCM and PG spectral methods reach to the error $\mathcal{O}(10^{-6})$ in half a second. Finally, Table 5.1 shows that the FSCM and the PG spectral method perform almost equivalently in solving (5.2). However, we note that in this case, the linear system resulting from the PG spectral method is diagonal. Therefore, in contrast to FSCM, the employment of the PG spectral method in other problems such as linear FPDEs and multiterm FPDEs becomes computationally more expensive due to the extra cost of quadrature, while possessing exponential accuracy.

REFERENCES

[1] E. BARKAI, R. METZLER, AND J. KLAFTER, *From continuous time random walks to the fractional Fokker-Planck equation*, Phys. Rev. E, 61 (2000), pp. 132–138.

[2] D. A. BENSON, S. W. WHEATCRAFT, AND M. M. MEERSCHAERT, *Application of a fractional advection-dispersion equation*, Water Resources Res., 36 (2000), pp. 1403–1412.

[3] L. BLANK, *Numerical Treatment of Differential Equations of Fractional Order*, Manchester Centre for Computational Mathematics, University of Manchester, UK, 1996.

[4] J. P. BOUCHAUD AND A. GEORGES, *Anomalous diffusion in disordered media: Statistical mechanisms, models and physical applications*, Phys. Rep., 195 (1990), pp. 127–293.

[5] W. CHESTER, *Resonant oscillations in closed tubes*, J. Fluid Mech, 18 (1964), pp. 44–64.

[6] K. DIETHELM AND N. J. FORD, *Analysis of fractional differential equations*, J. Math. Anal. Appl., 265 (2002), pp. 229–248.

[7] K. DIETHELM, N. J. FORD, AND A. D. FREED, *Detailed error analysis for a fractional Adams method*, Numer. Algorithms, 36 (2004), pp. 31–52.

[8] R. GORENFLO, F. MAINARDI, D. MORETTI, AND P. PARADISI, *Time fractional diffusion: A discrete random walk approach*, Nonlinear Dynam., 29 (2002), pp. 129–143.

[9] B. GUSTAFSSON, H. O. KREISS, AND J. OLIGER, *Time Dependent Problems and Difference Methods*, Wiley, New York, 1995.

[10] B. HENRY AND S. WEARNE, *Fractional reaction-diffusion*, Phys. A, 276 (2000), pp. 448–455.

[11] J. S. HESTHAVEN, S. GOTTLIEB, AND D. GOTTLIEB, *Spectral Methods for Time-Dependent Problems*, Cambridge Monogr. Appl. Comput. Math. 21, Cambridge University Press, Cambridge, UK, 2007.

[12] G. E. Karniadakis and S. J. Sherwin, *Spectral/hp Element Methods for CFD*, 2nd ed., Oxford University Press, New York, 2005.
[13] J. J. Keller, *Propagation of simple non-linear waves in gas filled tubes with friction*, Z. Angew. Math. Phys., 32 (1981), pp. 170–181.
[14] M. M. Khader, *On the numerical solutions for the fractional diffusion equation*, Commun. Nonlinear Sci. Numer. Simul., 16 (2011), pp. 2535–2542.
[15] M. M. Khader and A. S. Hendy, *The approximate and exact solutions of the fractional-order delay differential equations using Legendre pseudospectral method*, Inter. J. Pure Appl. Math., 74 (2012), pp. 287–297.
[16] R. Klages, G. Radons, and I. M. Sokolov, *Anomalous Transport: Foundations and Applications*, Wiley-VCH, Weinheim, Germany, 2008.
[17] T. Langlands and B. Henry, *The accuracy and stability of an implicit solution method for the fractional diffusion equation*, J. Comput. Phys., 205 (2005), pp. 719–736.
[18] R. J. LeVeque, *Finite Volume Methods for Hyperbolic Problems*, Cambridge Texts in Appl. Math. 31, Cambridge University Press, Cambridge, UK, 2002.
[19] X. Li and C. Xu, *A space-time spectral method for the time fractional diffusion equation*, SIAM J. Numer. Anal., 47 (2009), pp. 2108–2131.
[20] X. Li and C. Xu, *Existence and uniqueness of the weak solution of the space-time fractional diffusion equation and a spectral method approximation*, Commun. Comput. Phys., 8 (2010), pp. 1016–1051.
[21] Y. Lin and C. Xu, *Finite difference/spectral approximations for the time-fractional diffusion equation*, J. Comput. Phys., 225 (2007), pp. 1533–1552.
[22] F. Liu, M. M. Meerschaert, R. J. McGough, P. Zhuang, and Q. Liu, *Numerical methods for solving the multi-term time-fractional wave-diffusion equation*, Fract. Calc. Appl. Anal., 16 (2013), pp. 9–25.
[23] C. Lubich, *On the stability of linear multistep methods for Volterra convolution equations*, IMA J. Numer. Anal., 3 (1983), pp. 439–465.
[24] C. Lubich, *Discretized fractional calculus*, SIAM J. Math. Anal., 17 (1986), pp. 704–719.
[25] R. L. Magin, *Fractional Calculus in Bioengineering*, Begell House, Redding, CT, 2006.
[26] F. Mainardi, *Fractional Calculus and Waves in Linear Viscoelasticity: An Introduction to Mathematical Models*, Imperial College Press, London, 2010.
[27] R. Metzler and J. Klafter, *The random walk's guide to anomalous diffusion: A fractional dynamics approach*, Phys. Rep., 339 (2000), pp. 1–77.
[28] I. Podlubny, *Fractional Differential Equations*, Academic Press, San Diego, CA, 1999.
[29] J. M. Sanz-Serna, *A numerical method for a partial integro-differential equation*, SIAM J. Numer. Anal., 25 (1988), pp. 319–327.
[30] N. Sugimoto, *Burgers equation with a fractional derivative: Hereditary effects on nonlinear acoustic waves*, J. Fluid Mech., 225 (1991), pp. 631–653.
[31] N. Sugimoto and T. Kakutani, *Generalized Burgers' equation for nonlinear viscoelastic waves*, Wave Motion, 7 (1985), pp. 447–458.
[32] Z. Sun and X. Wu, *A fully discrete difference scheme for a diffusion-wave system*, Appl. Numer. Math., 56 (2006), pp. 193–209.
[33] M. Zayernouri and G. E. Karniadakis, *Fractional Sturm-Liouville eigen-problems: Theory and numerical approximations*, J. Comput. Phys., 47 (2013), pp. 2108–2131.
[34] M. Zayernouri and G. E. Karniadakis, *Exponentially accurate spectral and spectral element methods for fractional ODEs*, J. Comput. Phys., 257 (2014), pp. 460–480.
[35] O. C. Zienkiewicz, R. L. Taylor, and J. Z. Zhu, *The Finite Element Method: Its Basis and Fundamentals*, Butterworth-Heinemann, London, 2005.